# Hydraulic Conductivity Inverse Problem Using Richards Equation

**Rowan Cockett**
Department of Earth and Ocean Science
University of British Columbia
rcockett@eos.ubc.ca

## 1 Introduction & Motivation

Studying the processes that occur in the vadose zone, the region between the earth's surface and the fully saturated zone, is of critical importance for the understanding of our groundwater resources. The majority of groundwater recharge is derived through water that percolates through the vadose zone. As such, much attention has been given to monitoring and describing processes that occur in this region of the earth. Hydraulic conductivity is a property of the soil media and is the main regulator of groundwater flow. However, in many field investigations the hydraulic conductivity is often unknown or only known as a bulk average at various distinct points. As hydraulic conductivity is the main parameter of interest, an accurate estimate that is spatially consistent with the media is highly valuable. In saturated aquifers pumping-tests and slug-tests inject or extract water and measure the response of hydraulic-head, which is related to the hydraulic conductivity. The parameter estimates are a volume-average of the aquifer and the extent of the measurement varies proportionally to the volume of water injected or extracted in the test. The radial extent from a tested well can vary over several orders of magnitude from $10^{-1}$m in slug tests to $10^{3}$m in multi-day pumping tests. It is more complicated to estimate hydraulic conductivity in unsaturated media because the hydraulic conductivity is a function of saturation. Field tests include infiltration experiments where the goal is to saturate the soil to remove the dependence on saturation. These infiltration experiments typically do not fully saturate the soil and as such can consistently underestimate the saturated hydraulic conductivity. Laboratory experiments on core-samples are also regularly completed but are expensive, time-consuming, and average a small portion of the media that may not be representative.

The measurements and tests for hydraulic conductivity typically done in a hydrogeologic field investigation yield point-measurements that are bulk averages of the media. With only a small amount of data, groundwater models can often be over simplifications of the true process, which limits their usability. Geophysical methods can provide additional data that is spatially and temporally extensive. This data, however, is not a direct measurement of the hydrogeologic parameters of interest and must be processed in such a way that it is usable to hydrologists.

Time-lapse monitoring activities, such as in *Pidlisecky et al.* [2012], allow for comprehensive estimates of soil electrical conductivity (EC) in the vadose zone using DC-resistivity probes. In this study, an infiltration experiment is conducted to artificially recharge an aquifer in an agricultural area that has high pumping rates for irrigation. The infiltration experiment is monitored with the DC-resistivity probes and the estimates of EC are able to image the infiltration front and provide estimates of saturation through an empirical relation [*Archie*, 1942]. The rate and variation of the infiltration front is a function of the porous media and as such can provide estimates of hydraulic properties, such as hydraulic conductivity. In this paper I will investigate a few of the initial steps necessary to use geophysical methods to invert for hydraulic conductivity.

The work completed in this paper will use pressure-head data to invert for saturated hydraulic conductivity using the groundwater flow equations in unsaturated media. The inversion will require a forward model that simulates unsaturated flow through time. Additionally, the sensitivity of the flow to perturbations in hydraulic conductivity must be calculated. This paper will: (a) implement, describe, and test the forward model for unsaturated groundwater flow

using Richards equation; (b) describe the inversion process that is used to estimate hydraulic conductivity; (c) outline the future steps that are needed to fully couple the geophysics and the hydrogeologic models.

## 2 Background

### 2.1 Richards Equation

Flow in the vadose zone has many complications as the parameters that control the flow are dependent on the saturation of the media, leading to a non-linear problem. Flow in the vadose zone is referred to as unsaturated flow, and is described by Richards equation. The groundwater flow equation has a diffusion term, as well as an advection term that is related to gravity and only acts in the $z$-direction. There are two different forms of Richards equation that will be considered in this paper that differ on how they deal with the non-linearity in the time-stepping term. The most fundamental form is called the mixed form of Richards Equation [*Celia et al.*, 1990]:

$$\frac{\partial \theta(\psi)}{\partial t} - \nabla \cdot K(\psi) \nabla \psi - \frac{\partial K(\psi)}{\partial z} = 0 \tag{1}$$

where $\theta$ is water content, and $\psi$ is pressure head. This formulation of Richards equation is called the 'mixed'-form because the equation is parameterized in $\psi$ but the time-stepping is in terms of $\theta$. The most commonly used formulation of Richards equation is known as the head-based form, and is popular because the time-stepping is explicitly written in terms of $\psi$.

$$C(\psi)\frac{\partial \psi}{\partial t} - \nabla \cdot K(\psi) \nabla \psi - \frac{\partial K(\psi)}{\partial z} = 0 \tag{2}$$

where $C(\psi) = \frac{\partial \theta}{\partial \psi}$ and is called the specific moisture capacity function. The differences in discretization and benefits in choosing between these two formulations will be discussed in detail in this paper.

An important aspect of unsaturated flow is noticing that both water content and hydraulic conductivity are functions of pressure-head ($\psi$). There are many empirical relations used to relate these parameters, including the Brooks-Corey model and the Van Genuchten model [*van Genuchten*, 1980]. The Van Genuchten model is slightly more popular when modeling because there are no discontinuities in the functions, unlike the Brooks-Corey model. A version of the Van Genuchten model is written [*Celia et al.*, 1990]:

$$\theta(\psi) = \frac{\alpha(\theta_s - \theta_r)}{\alpha + |\psi|^\beta} + \theta_r \tag{3a}$$

$$K(\psi) = K_s \frac{A}{A + |\psi|^\gamma} \tag{3b}$$

Where parameters $\alpha$, $\beta$, $\gamma$, and $A$ are fitting parameters that are often assumed to be constant in the media; $\theta_r$ and $\theta_s$ are the residual and saturated moisture contents; and $K_s$ is the saturated hydraulic conductivity. An example of the curves using Van Genuchten parameters from *Celia et al.* [1990] is shown in Figure 1. Small changes in pressure head can change the hydraulic conductivity several orders of magnitude; as such, $K(\psi)$ is a highly nonlinear function. The water content curve is also highly nonlinear as saturation can change dramatically over a small range of pressure head values (Figure 1). It should be noted that these functions are only valid when the pressure-head $\psi$ is negative; that is, the media is semi-saturated. When the media is fully saturated $K = K_s$ and $\theta$ is equal to the porosity.

Typical uses of Richards equation are to simulate infiltration experiments in both the laboratory and the field scale. These experiments begin with an initially dry soil and then add water to the top of the core sample (or ground surface). The simulation of this experiment requires simulating fast changes in pressure head and saturation over the most nonlinear part of the Van Genuchten curves. This experiment is the motivation for the discretization scheme that is described in the following section.

## 3 Discretization

Richards equation is parameterized in terms of pressure head ($\psi$) in both the mixed- and the head-based forms. This paper describes simulating Richards equation for one-, two-, and three-dimensions, however, special attention is paid to the one-dimensional case. The spatial discretization for Richards equation was chosen to be a finite-volume approximation; this is a natural extension of mass-conservation in a volume where the balance of fluxes into and out of a

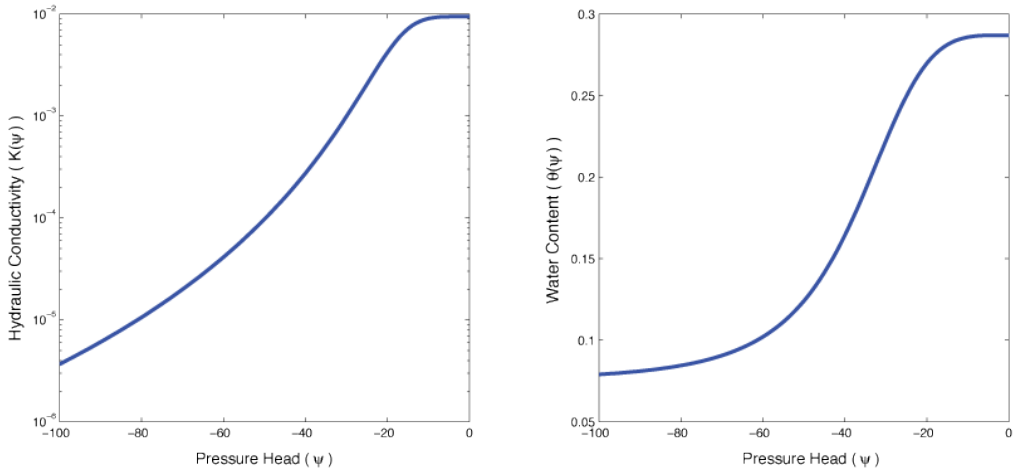


Figure 1: Example Van Genuchten curves for (a) hydraulic conductivity and (b) water content. Parameters used from Equation 3 are $\alpha = 1.611 \times 10^6$, $\theta_s = 0.287$, $\theta_r = 0.075$, $\beta = 3.96$, $A = 1.175 \times 10^6$, $\gamma = 4.74$, $K_s = 9.44 \times 10^{-5}$ m/s.

volume is conserved. In two-dimensions the flux into and out of a volume can be seen in Figure 2. Here it is natural to assign the entire cell one hydraulic conductivity value, which is located at the cell center. Assigning the cell-center the value for hydraulic conductivity, rather than a cell face or node, has the interpretation that a single value fills the entire cell and allows for discontinuities between adjacent cells. From a geologic perspective discontinuities are prevalent, as you can have large differences in hydraulic properties between layers in the ground. The pressure-head data will also be located at the cell centers. The discretization chosen results in a staggered mesh in space. The details of the spatial and temporal discretization will be outlined in the following two sections.

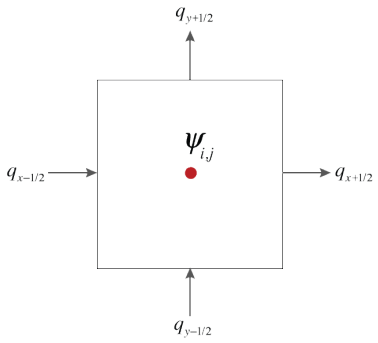


Figure 2: Finite volume grid in 2D showing flux into and out of a single cell.

### 3.1 Spatial Discretization

Richards equation is discretized on a cell-centered finite volume mesh, and the discrete approximation will be explicitly written for one-dimension. Ignoring the discretization of the time derivative, Richards equation can be written in matrix form:

$$\frac{\partial\theta(\psi)}{\partial t} - \mathbf{D}\,\mathrm{diag}\left(\frac{1}{\mathbf{A}_v \frac{1}{K(\psi^{n+1})}}\right)\mathbf{G}\psi - \mathbf{D}_z\left(\frac{1}{\mathbf{A}_v \frac{1}{K(\psi^{n+1})}}\right) = 0 \tag{4}$$

Here $\mathbf{D}$ and $\mathbf{G}$ are the discretized divergence and gradient operators, respectively. The derivative in the $z$-direction is written $\mathbf{D}_z$, and in one-dimension is the same as the divergence matrix. The gradient operator, $\mathbf{G}$, takes the parameters at cell-centers and yields values at cell-faces ($\mathbb{R}^n \to \mathbb{R}^{n+1}$). The values of $\psi$ and $K(\psi)$ are known on the cell-centers (Figure 3) and must first be averaged to the cell faces; this is completed through harmonic averaging. The ends of the mesh ($\psi_1$ and $\psi_N$) are extrapolated to the cell-faces using nearest-neighbour extrapolation.

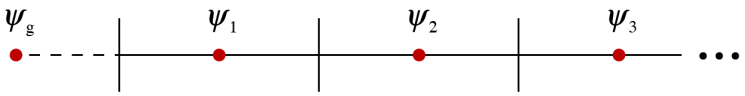


Figure 3: Cell centered mesh in one-dimension showing a ghost-point

The gradient operator, $\mathbf{G}$, uses a first-order finite-difference approximation. Inhomogeneous Dirichlet boundary conditions are incorporated using a ghost-point outside of the mesh (Figure 3). The value at the boundary face is given by the average $\psi_{\frac{1}{2}} = \frac{1}{2}(\psi_1 + \psi_g)$, which can be put into matrix $\mathbf{G}$ by eliminating $\psi_g$.

$$\mathbf{G}\psi = \frac{1}{h}\underbrace{\begin{bmatrix} 2 & & & & \\ -1 & 1 & & & \\ & \ddots & \ddots & & \\ & & & -1 & 1 \\ & & & & -2 \end{bmatrix}}_{\text{Gradient matrix}}\begin{bmatrix} \psi_1 \\ \psi_2 \\ \vdots \\ \psi_{N-1} \\ \psi_N \end{bmatrix} + \underbrace{\frac{1}{h}\begin{bmatrix} -2 & 0 \\ 0 & 0 \\ \vdots & \vdots \\ 0 & 0 \\ 0 & 0 \\ 0 & 2 \end{bmatrix}\begin{bmatrix} \psi_{\frac{1}{2}} \\ \psi_{N+\frac{1}{2}} \end{bmatrix}}_{\text{Inhomogeneous dirichlet boundary condition matrix}} \tag{5}$$

If the boundary conditions are homogeneous Dirichlet ($\psi_{\frac{1}{2}} = \psi_{N+\frac{1}{2}} = 0$) the boundary condition matrix may be dropped. If homogeneous Neumann (no-flux) boundary conditions are needed, the gradient at the boundary face is known to be zero, so this value can be included by a row of zeros in the gradient matrix. The divergence matrix, $\mathbf{D}$ operates from $\mathbb{R}^{n+1} \to \mathbb{R}^n$ and no boundary conditions are considered. The divergence matrix is a simple first-order difference approximation that yields the values at cell-centers. For a non-regular mesh where $\exists i, j : h_i \neq h_j$ changes in the mesh size must be accounted for in the gradient and divergence matrices. The non-regular mesh has been implemented but will not be discussed in more detail here.

To move to higher dimensions in a tensor-product mesh, Kronecker products may be used to place the finite-difference on the correct cells. For example, the gradient matrix in three-dimensions may be formed by:

$$\begin{aligned} \mathbf{G}_x &= \mathbf{I}_3 \otimes (\mathbf{I}_2 \otimes \mathbf{G}_1) \\ \mathbf{G}_y &= \mathbf{I}_3 \otimes (\mathbf{G}_2 \otimes \mathbf{I}_1) \\ \mathbf{G}_z &= \mathbf{G}_3 \otimes (\mathbf{I}_2 \otimes \mathbf{I}_1) \end{aligned} \tag{6}$$

where $\mathbf{G}_n$ is the gradient operator in one-dimension for the $n^{\text{th}}$ dimension. The $\mathbf{I}_n$ is the identity matrix that has the size of the mesh in the $n^{\text{th}}$ dimension. Here the full gradient operator can be formed by $\mathbf{G} = [\mathbf{G}_x^\top \quad \mathbf{G}_y^\top \quad \mathbf{G}_z^\top]^\top$. The divergence, and averaging matrices can also be formed using Kronecker products, where $\mathbf{D} = [\mathbf{D}_x \quad \mathbf{D}_y \quad \mathbf{D}_z]$. By focusing on the form of the finite-difference matrices in one-dimension, one can rapidly extend the implementation to simulate two- and three-dimensions.

The gradient and divergence operators are both second-order accurate, due to the staggered mesh implementation. The order of accuracy can be tested on analytic functions where the derivative is known. Testing has been completed in one, two, and three dimensions and shows a decrease of $\mathcal{O}(\delta^2)$ for regular as well as non-regular meshes.

### 3.2 Time Discretization

Richards equation is often used to simulate water infiltrating into an initially dry soil. At early times in an infiltration experiment the pressure head ($\psi$) can be close to discontinuous. These large changes in $\psi$ are also reflected in the non-

linear terms $K$ and $\theta$; as such, the initial conditions imposed can severely limit the step-size in time if an inappropriate time discretization is chosen. Hydrogeologists are often interested in the process until steady-state is achieve, which may take many time-steps. Considerations of stiffness and length of the time integration point to a numerical scheme that is not limited by stiffness. In this paper I will describe the implementation of a fully-implicit backward Euler numerical scheme for both the mixed- and head-based formulation (Eq. 1 & Eq. 2). Higher order implicit methods are not considered here because the uncertainty associated with the fitting parameters in the Van Genuchten models (Eq. 3) have much more effect than the order of the numerical method used. The discretized approximation to the mixed-form of Richards equation using fully-implicit backward Euler is:

$$F(\psi^{n+1}, \psi^n) = \frac{\theta(\psi^{n+1}) - \theta(\psi^n)}{\Delta t} - \mathbf{D}\,\mathrm{diag}\left(\frac{1}{\mathbf{A}_v \frac{1}{K(\psi^{n+1})}}\right)\mathbf{G}\psi^{n+1} - \mathbf{D}_z\left(\frac{1}{\mathbf{A}_v \frac{1}{K(\psi^{n+1})}}\right) = 0 \tag{7}$$

To satisfy Richards equation, $F(\psi^{n+1}, \psi^n) = 0$ at the correct $\psi^{n+1}$. However, because of the nonlinearity it is not possible to directly solve for $\psi^{n+1}$ and an iterative update must be solved for at every time-step. Additionally, the update $\psi^{n+1}$ is contained inside the function for moisture content ($\theta$). To deal with the non-linearity many numerical solutions for Richards equation use the chain rule to separate $\frac{\partial\theta}{\partial t}$ into $\frac{\partial\theta}{\partial\psi}\frac{\partial\psi}{\partial t}$ where $\frac{\partial\theta}{\partial\psi}$ is known from the analytic function in Equation 3.

### 3.2.1 Head-Based Form

The chain-rule splitting of the time derivative results in the so-called head-based form of Richards equation. Although the splitting of this derivative into components is equivalent in the continuous domain, the discretized version is not and the method may not be conservative [*Celia et al.*, 1990]. However, this method has been historically prevalent in the hydrogeology literature (e.g. *Brunone et al.* [1998]; *Miller et al.* [1998]). Isolating $\frac{\partial\psi}{\partial t}$ allows a Picard iteration ($m = 1, 2, \dots$) to be performed:

$$C(\psi^{n+1,m})\frac{\psi^{n+1,m+1} - \psi^n}{\Delta t} - \mathbf{D}\,\mathrm{diag}\left(K_{Av}^{n+1,m}\right)\mathbf{G}\psi^{n+1,m+1} - \mathbf{D}_z K_{Av}^{n+1,m} = R_P^{n+1,m} \tag{8}$$

where $K_{Av}^{n+1,m} = (\mathbf{A}_v K^{-1}(\psi^{n+1,m}))^{-1}$ and $C(\psi) = \frac{\partial\theta}{\partial\psi}$ and is commonly referred to as the specific moisture capacity function. This equation may be solved for the update to the pressure head $\delta\psi = \psi^{n+1,m+1} - \psi^{n+1,m}$ by rewriting Equation 8.

$$\left(\frac{C(\psi^{n+1,m})}{\Delta t} - \mathbf{D}\,\mathrm{diag}\left(K_{Av}^{n+1,m}\right)\mathbf{G}\right)\delta\psi = \mathbf{D}\,\mathrm{diag}\left(K_{Av}^{n+1,m}\right)\mathbf{G}\psi^{n+1,m} + \mathbf{D}_z K_{Av}^{n+1,m} - C(\psi^{n+1,m})\frac{\psi^{n+1,m} - \psi^n}{\Delta t} \tag{9}$$

The update to the pressure head, $\delta\psi$, can now be found by solving this linear system and updating

$$\psi^{n+1,m+1} = \psi^{n+1,m} + \delta\psi \tag{10}$$

until the residual between inner iterations is sufficiently close to zero. After the Picard iteration is complete $\psi^{n+1}$ is set to the final iterate $\psi^{n+1,m+1}$ and the next time-step can be performed.

### 3.2.2 Mixed Form - Picard Iteration

The nonconservative nature of the head-based form of Richards equation led *Celia et al.* [1990] to propose the mixed form of the equation. The mixed form does not separate the continuous form of the Richards equation but instead expands using a Taylor series about the $m^{\text{th}}$ iterate of $\theta$ to approximate $\psi^{n+1,m+1}$.

$$\frac{\theta^{n+1,m+1} - \theta^n}{\Delta t} = \frac{\theta^{n+1,m} + \left.\frac{\partial\theta}{\partial\psi}\right|^{n+1,m}\delta\psi - \theta^n}{\Delta t} + \mathcal{O}(\delta^2) \tag{11}$$

The Taylor series can be linearized and substituted into the mixed form of Richards equation. Rearranging the equation for $\delta\psi$ results in:

$$\left(\frac{C(\psi^{n+1,m})}{\Delta t} - \mathbf{D}\,\mathrm{diag}\left(K_{Av}^{n+1,m}\right)\mathbf{G}\right)\delta\psi = \mathbf{D}\,\mathrm{diag}\left(K_{Av}^{n+1,m}\right)\mathbf{G}\psi^{n+1,m} + \mathbf{D}_z K_{Av}^{n+1,m} - \frac{\theta^{n+1,m} - \theta^n}{\Delta t} \tag{12}$$

This is a very similar to the head-based formulation, and can be solved in a similar way using the Picard iteration and updating $\psi^{n+1,m+1} = \psi^{n+1,m} + \alpha\delta\psi$. The only difference between the head-based form and the mixed-form is in the last term which approximates the time derivative in $\theta$. The mixed-formulation has been shown to be mass conservative *Celia et al.* [1990] and is a superior numerical scheme to the head-based formulation. The Picard iteration, however, may take many iterations to converge and each inner iteration requires solving a linear system of equations. The slow convergence of this fixed-point iteration motivates a more sophisticated root-finding algorithm.

### 3.2.3 Mixed Form - Newton Iteration

Using a Newton root-finding method can decrease the number of iterations necessary without significantly increasing the size or complexity of the linear system to be solved. The Newton root-finding method iterates over $m = 1, 2, \ldots$ and can be written $F(\psi^{n+1,m}, \psi^n) = R_N^{n+1,m}$ (Eq. 7), where $R_N^{n+1,m}$ is the Newton residual. For Newton root-finding the Jacobian of the system is necessary; the derivative of $F(\psi^{n+1,m}, \psi^n)$ with respect to $\psi^{n+1,m}$ is

$$J_{\psi^{n+1,m}} = \frac{1}{\Delta t}\frac{\partial\theta(\psi^{n+1,m})}{\partial\psi^{n+1,m}} - \frac{\partial}{\partial\psi^{n+1,m}}\left(\mathbf{D}\,\mathrm{diag}\left(K_{Av}^{n+1,m}\right)\mathbf{G}\psi^{n+1,m}\right) - \mathbf{D}_z\frac{\partial K_{Av}^{n+1,m}}{\partial\psi^{n+1,m}} \tag{13a}$$

$$\frac{\partial}{\partial\psi}\left(\mathbf{D}\,\mathrm{diag}\left(K_{Av}\right)\mathbf{G}\psi\right) = \mathbf{D}\,\mathrm{diag}\left(K_{Av}\right)\mathbf{G} + \mathbf{D}\,\mathrm{diag}\left(\mathbf{G}\psi\right)\frac{\partial K_{Av}}{\partial\psi} \tag{13b}$$

$$\frac{\partial K_{Av}}{\partial\psi} = \mathrm{diag}\left(\left(\mathbf{A}_v K^{-1}(\psi)\right)^{-2}\right)\mathbf{A}_v\,\mathrm{diag}\left(K^{-2}(\psi)\right)\frac{\partial K(\psi)}{\partial\psi} \tag{13c}$$

Here the analytical derivatives of the Van Genuchten equations are needed. It should be noted that when $\psi$ is a vector these derivatives are diagonal matrices.

$$C(\psi) = \frac{\partial\theta}{\partial\psi} = -\frac{\alpha(\theta_s - \theta_r)}{(\alpha + |\psi|^\beta)^2}\beta|\psi|^{\beta-1}\mathrm{sign}(\psi) \tag{14a}$$

$$\frac{\partial K}{\partial\psi} = -K_s\frac{A}{(A + |\psi|^\gamma)^2}\gamma|\psi|^{\gamma-1}\mathrm{sign}(\psi) \tag{14b}$$

To have a fully inplicit scheme, the update to $n+1$ requires a non-linear solve. This is completed by using a Newton root finding technique.

$$F(\psi^{n+1,m} + \delta\psi, \psi^n) = F(\psi^{n+1,m}, \psi^n) + J_{\psi^{n+1,m}}\delta\psi + \mathcal{O}(\delta^2) \tag{15}$$

so the update $\partial\psi$ can be found by linearizing, setting Equation 15 to zero, and solving the linear system

$$\delta\psi = -J_{\psi^{n+1,m}}^{-1}F(\psi^{n+1,m}, \psi^n) \tag{16}$$

The iteration is completed by adding the Newton update to the last iterate

$$\psi^{n+1,m+1} = \psi^{n+1,m} + \alpha\delta\psi \tag{17}$$

The pure Newton step may also overshoot the root; to prevent this, a simple back-tracking linesearch is used to ensure a sufficient decrease in $R_N^{n+1,m}$. The Newton root-finding method must solve a linear system of an equal size to the Picard iteration. However, when the initial guess is close to the actual solution (i.e. $\psi^n$ is close to $\psi^{n+1}$) the Newton method converges quadratically, reducing the number of times the linear system must be solved. It is noted that the Jacobian may have negative eigenvalues, which will cause the root-finding algorithm to diverge. The implementation often fails when the boundary conditions are not honored in the initial conditions or the conditions in the soil column are discontinuous and changing rapidly. If the Newton iteration fails to converge to a solution the update is performed with the less efficient but equivalent mixed-form Picard iteration discussed above.

## 4 Code Testing

Richards equation has no analytic solution, which makes rigorous testing of the code more involved. In the following section I will detail a comparison to a well documented literature example which provides qualitative agreement. For a more rigorous testing of the code, a fictitious source test is completed and is described below.

### 4.1 Comparison to Literature

*Celia et al.* [1990] provides a full numerical example with detailed boundary conditions and Van Genuchten parameters. As an initial test of the code described in this paper, a comparison with *Celia et al.* [1990] is provided. The parameters for the Van Genuchten equations (Eq. 3) are $\alpha = 1.611 \times 10^6$, $\theta_s = 0.287$, $\theta_r = 0.075$, $\beta = 3.96$, $A = 1.175 \times 10^6$, $\gamma = 4.74$, $K_s = 9.44 \times 10^{-5}$ m/s [*Celia et al.*, 1990]. The initial conditions of a 40cm high 1D soil column are initially dry with a pressure head $\psi_0(x, 0) = -61.5$cm. The boundary conditions applied are inhomogeneous Dirichlet with the top of the soil column $\psi(40\text{cm}, t) = -20.7$cm, and the bottom of the soil column $\psi(0\text{cm}, t) = -61.5$cm. The initial conditions are not consistent with the boundary conditions, and as such a steep gradient in the pressure head is setup. The spatial grid is regular and as a spacing of 0.5cm, the time stepping has a $\Delta t = 1$s. The solution at 360s obtained with the Newton algorithm presented is compared to the 'Dense Grid' solution obtained in *Celia et al.* [1990], and in presented in Figure 4. Comparing the results obtained from the two algorithms shows good agreement; however, as the data is not provided it is impossible to evaluate quantitative agreement between the solutions.

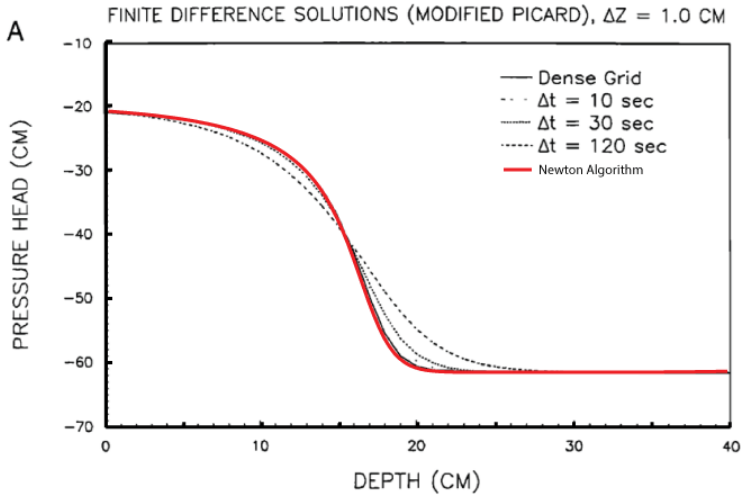


Figure 4: Comparison at $t$ =360s of presented algorithm to the solution in *Celia et al.* [1990] using a modified Picard iteration. (Adapted from *Celia et al.* [1990])

### 4.2 Fictitious Source

We use a fictitious source experiment to rigorously test the code. In this experiment we will approximate an infiltration front by an arctangent function centered over the highly nonlinear part of the Van Genuchten curves in Figure 1. The arctangent curve advects into the soil column with time. The advantage of using an analytic function is that the derivative is known explicitly and can be calculated at all times. However, it should be noted that Richards equation does not satisfy the analytic solution exactly, but differs by a function $S(x, t)$; this function is referred to as the fictitious source term. The analytic function used has similar boundary conditions and shape to the previous example, and is considered over the domain $x \in [0, 1]$.

$$\Psi_{\text{true}}(x, t) = -20 \arctan(20((x - 0.25) - t)) - 40 \tag{18}$$

This analytic function is shown at time 0 and time 0.5 in Figure 5 and has a pressure head range of $\psi \in [-60, -20]$; these values can be directly compared to the Van Genuchten curves in Figure 1. The known pressure head can then be put directly into Richards equation (Eq. 1) and the analytic derivatives can be calculated and equated to a source term $S(x, t)$. Knowing this source term and the analytic boundary conditions the discretized form of Richards equation can be solved, and should reproduce the analytic function in Equation 18. Table 1 shows the results of the fictitious source test when the number of mesh-cells is doubled; the time-discretization is fixed and is the same as the mesh size (i.e. $k = h$). In this case it is expected that the order of accuracy should be limited by the backward-Euler time discretization, which is $\mathcal{O}(\delta)$. The final column of Table 1 indeed shows that the order of accuracy is $\mathcal{O}(\delta)$. The higher

errors in the coarse discretization is due to the high discontinuities and changes in the source term, which the coarse discretizations do not resolve. A similar procedure can be completed in two and three dimensions, and these tests also show the same results. The rigorous testing of the code presented provides confidence in the results that are described in the following sections of this paper.

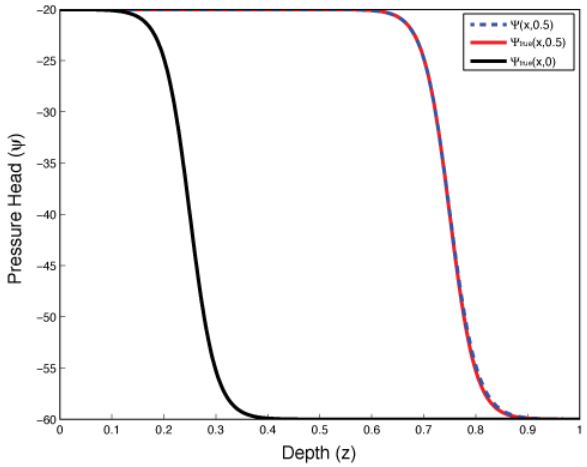


Figure 5: Ficticious source test in 1D showing the analytic function $\Psi_{\text{true}}$ at times 0.0 and 0.5 and the numerical solution $\Psi(x, 0.5)$ using the mixed-form Newton iteration

Table 1: Ficticious Source Test in 1D using the mixed-form Newton iteration

| Mesh Size (n) | $\|\|\Psi(x,0.5) - \Psi_{\text{true}}(x,0.5)\|\|_\infty$ | Order Decrease |
|---|---|---|
| 64 | 5.485569e+00 | |
| 128 | 2.952912e+00 | 0.894 |
| 256 | 1.556827e+00 | 0.924 |
| 512 | 8.035072e-01 | 0.954 |
| 1024 | 4.086729e-01 | 0.975 |
| 2048 | 2.060448e-01 | 0.988 |
| 4096 | 1.034566e-01 | 0.994 |
| 8192 | 5.184507e-02 | 0.997 |

## 5 Inverse Problem

The location and spatial variability of an infiltration front over time is inherently dependent on the hydraulic properties of the soil column. As such, taking measurements of the saturation or pressure head at various depths along a soil profile should contain information about the soil properties. The inverse problem that is framed here is the estimation of saturated hydraulic conductivity from pressure head data at a few locations in the soil column. The data for this problem comes from the simulation of vadose zone flow described above using Richards equation. Pressure heads are simulated at all locations in the soil column, but are only recorded at a few locations. This is completed by multiplying the full pressure head data vector (all locations and times) by a projection matrix $\mathbf{Q}$. For example, if data is recorded at two locations in soil column, the projection matrix would have the form:

$$\mathbf{Q} = \begin{bmatrix} 0 & \dots & 0 & 1 & 0 & \dots & & 0 \\ 0 & & \dots & & 0 & 1 & 0 \dots & 0 \end{bmatrix} \otimes \mathbf{I} \tag{19}$$

Here $\mathbf{I} \in \mathbb{R}^{n_t \times n_t}$ where $n_t$ is the number of time steps. It is now possible to simulate recorded data using the solution to Richards equation.

$$\mathbf{d}(\mathbf{m}) = \mathbf{Q}\boldsymbol{\Psi}(\mathbf{m}) \tag{20}$$

Where $\mathbf{m}$ is the model for the hydraulic properties and may include saturated hydraulic conductivity and other Van Genuchten parameters. The data collected depends on the hydraulic parameters of the soil, as such, the inverse can now be formulated by defining the objective function to be minimized.

### 5.1 Objective Function

The inversion for hydraulic conductivity results in an unconstrained non-linear optimization problem that is underdetermined; that is, observational data is much fewer than the number of model parameters. Due to the inverse problem being underdetermined, a weighted regularization parameter is generally added to the optimization problem and the two-part function is minimized.

$$\Phi(\mathbf{m}) = \frac{1}{2}\left\|\mathbf{W}(\mathbf{d}(\mathbf{m}) - \mathbf{d_{obs}})\right\|_2^2 + \frac{\beta}{2}\|\mathbf{G_w}(\mathbf{m} - \mathbf{m_{ref}})\|_2^2 \tag{21}$$

Here the first term minimizes data-misfit between the generated data, $\mathbf{d}(\mathbf{m})$, and the observed data ($\mathbf{d_{obs}}$). In the current application a $l^2$-norm was chosen to characterize this misfit. The second term is a Tikhonov style term that controls model regularization with regard to a reference model ($\mathbf{m_{ref}}$) [*Tikhonov and Arsenin*, 1977]. $\mathbf{G_w}$ is a combination of a standard gradient operator, which is sensitive to model flatness; and the identity matrix, which is sensitive to model smallness. Both flatness and smallness are with respect to $\mathbf{m_{ref}}$. $\beta$ is a regularization parameter that balances the inversion between minimizing data-misfit and model regularization. When fitting the data in the objective function it is necessary to change the weight of the inversion so that it is equally sensitive to large and small data if they are valid. This data weighting is done by adding a weighting matrix to the data residual ($\mathbf{d_m} - \mathbf{d_{obs}}$). In Equation 21, $\mathbf{W}$ is a diagonal weighting matrix that is multiplied by the residual vector:

$$\mathbf{W} = \text{ diag}\left(\frac{1}{|\mathbf{d_{obs}}|\, SD(\mathbf{d_{obs}}) + \epsilon}\right) \tag{22}$$

where $SD(\mathbf{d_{obs}})$ is the element wise standard deviation of each data; $\epsilon$ is a small positive constant that ensures a cut-off value so an extremely large weight is not given to very low amplitude data. This operation is done element wise on the vector $\mathbf{d_{obs}}$ and the result is placed on the diagonal of the weighting matrix $\mathbf{W}$.

It is clear that regularization can play an important role in the construction of the objective function. The inclusion of *a priori* knowledge into the inversion can be completed by adjusting parameters such as $\mathbf{m_{ref}}$ to include the background conductivity or adjusting flatness regularization in different directions to agree with geologic assumptions.

To minimize the objective function, both the gradient and Hessian of Equation 21 are necessary. Here we approximate the Hessian of the objective function with only the first order terms that are guaranteed to be positive definite.

$$\nabla\Phi(\mathbf{m}) = \mathbf{J}^\top\mathbf{W}^\top\mathbf{W}(\mathbf{d}(\mathbf{m}) - \mathbf{d_{obs}}) + \beta\mathbf{G_w}^\top\mathbf{G_w}(\mathbf{m} - \mathbf{m_{ref}}) = \mathbf{g} \tag{23}$$

$$\nabla^2\Phi(\mathbf{m}) \approx \mathbf{J}^\top\mathbf{W}^\top\mathbf{W}\mathbf{J} + \beta\mathbf{G_w}^\top\mathbf{G_w} = \mathbf{H} \tag{24}$$

Here $\mathbf{J}$ is the Jacobian of the modeled data with respect to the hydraulic parameters ($\frac{\partial \mathbf{d}(\mathbf{m})}{\partial \mathbf{m}}$) and describes the sensitivity of data to changes in model parameters. The derivation of the Jacobian is described in the following section.

### 5.2 Richards Equation Derivative

For the inverse problem we must take the derivative of Richards equation to the parameters of interest. This will involve writing the whole time-stepping process as a block-matrix and taking the derivative. Richards equation can be written as a function of the model, and for one time-step is written:

$$F(\psi^{n+1}, \psi^n, m) = \frac{\theta^{n+1}(\psi^{n+1}) - \theta^n(\psi^n)}{\Delta t} - \nabla \cdot K(\psi^{n+1}, m)\nabla\psi^{n+1} - \frac{\partial}{\partial z}K(\psi^{n+1}, m) = 0 \tag{25}$$

In this case $m$ contains all the parameters of interest and is a vector. Here we note that $\psi^{n+1}$ and $\psi^n$ are also functions of $m$. The sensitivity of $F$ to the change in the parameters $m$ can be written:

$$\frac{\partial F(\psi^{n+1},\psi^n,m)}{\partial m} = \frac{1}{\Delta t}\left(\frac{\partial \theta^{n+1}}{\partial \psi^{n+1}}\frac{\partial \psi^{n+1}}{\partial m} - \frac{\partial \theta^n}{\partial \psi^n}\frac{\partial \psi^n}{\partial m}\right) - \nabla\cdot\ \text{diag}\left(\nabla\psi^{n+1}\right)\left(\frac{\partial K}{\partial m} + \frac{\partial K}{\partial \psi^{n+1}}\frac{\partial \psi^{n+1}}{\partial m}\right)$$
$$-\nabla\cdot K(\psi^{n+1})\nabla\frac{\partial \psi^{n+1}}{\partial m} - \frac{\partial}{\partial z}\left(\frac{\partial K}{\partial m} + \frac{\partial K}{\partial \psi^{n+1}}\frac{\partial \psi^{n+1}}{\partial m}\right) = 0 \quad (26)$$

It should be noted that if harmonic averaging is used for the $K$ this must also be taken into account in the derivative. Additionally, any inhomogeneous boundary conditions that are not contained in the discretized operators must also be included. In this case we are solving for $\frac{\partial \Psi}{\partial m}$ where $\Psi = [\psi_1, \psi_2, \ldots, \psi_n]^\top$. To do this we will rearrange the above equation into a block-matrix, where we can solve for $\frac{\partial \Psi}{\partial m}$.

$$\overbrace{\left[-\frac{1}{\Delta t}\frac{\partial \theta^n}{\partial \psi^n}\right]}^{\mathbf{A}_{-1}(\psi^n)}\frac{\partial \psi^n}{\partial m} + \overbrace{\left[\frac{1}{\Delta t}\frac{\partial \theta^n}{\partial \psi^{n+1}} - \nabla\cdot\ \text{diag}\left(\nabla\psi^{n+1}\right)\frac{\partial K}{\partial \psi^{n+1}} - \nabla\cdot K(\psi^{n+1})\nabla - \frac{\partial}{\partial z}\frac{\partial K}{\partial \psi^{n+1}}\right]}^{\mathbf{A}_0(\psi^{n+1})}\frac{\partial \psi^{n+1}}{\partial m}$$
$$= \underbrace{\nabla\cdot\ \text{diag}\left(\nabla\psi^{n+1}\right)\frac{\partial K}{\partial m} + \frac{\partial}{\partial z}\frac{\partial K}{\partial m}}_{\mathbf{b}(\psi^{n+1},m)} \quad (27)$$

Here the subscript notation of $\mathbf{A}_0(\psi^{n+1})$ and $\mathbf{A}_{-1}(\psi^n)$ represents the diagonal of the matrix $\mathbf{A}(\Psi, m)$. If $\psi_0$ does not depend on the parameters, then the matrix can be formulated as:

$$\overbrace{\begin{bmatrix} \mathbf{A}_0(\psi_1) & & & & & \\ \mathbf{A}_{-1}(\psi_1) & \mathbf{A}_0(\psi_2) & & & & \\ & \mathbf{A}_{-1}(\psi_2) & \mathbf{A}_0(\psi_3) & & & \\ & & \ddots & \ddots & & \\ & & & \mathbf{A}_{-1}(\psi_{n-1}) & \mathbf{A}_0(\psi_n) \end{bmatrix}}^{\mathbf{A}(\Psi,m)} \overbrace{\begin{bmatrix} \frac{\partial \psi_1}{\partial m} \\ \frac{\partial \psi_2}{\partial m} \\ \vdots \\ \frac{\partial \psi_{n-1}}{\partial m} \\ \frac{\partial \psi_n}{\partial m} \end{bmatrix}}^{\frac{\partial \Psi}{\partial m}} = \overbrace{\begin{bmatrix} \mathbf{b}(\psi_1, m) \\ \mathbf{b}(\psi_2, m) \\ \vdots \\ \mathbf{b}(\psi_{n-1}, m) \\ \mathbf{b}(\psi_n, m) \end{bmatrix}}^{\mathbf{B}(\Psi,m)} \quad (28)$$

Note here that this is a block matrix equation, and both the storage and solving will be expensive if it is computed all at once. It should be noted, however, that $\mathbf{J}$ is never needed only the products $\mathbf{J}\mathbf{v}$ and $\mathbf{J}^\top\mathbf{z}$ are needed.

$$\mathbf{J} = \mathbf{Q}\mathbf{A}(\Psi, m)^{-1}\mathbf{B}(\Psi, m) \quad (29)$$

Where $\mathbf{Q}$ is a projection from the full solution onto the data-space. To compute $\mathbf{J}\mathbf{v}$ we can use an intermediate step to solve for $\mathbf{y}$ in $\mathbf{A}\mathbf{y} = \mathbf{B}\mathbf{v}$ and then project onto the data-space by computing $\mathbf{Q}\mathbf{y}$. Similarly, to compute $\mathbf{J}^\top\mathbf{z}$ involves the intermediate solve for $\mathbf{y}$ in $\mathbf{A}^\top\mathbf{y} = \mathbf{Q}^\top\mathbf{z}$ and then computation of $\mathbf{B}^\top\mathbf{y}$. In this case, the matrix $\mathbf{A}(\Psi, m)$ does not even need to be explicitly formed because the matrix is a lower-triangular block-system, and can be solved using a forward substitution. Similarly, $\mathbf{A}^\top\mathbf{y} = \mathbf{Q}^\top\mathbf{z}$ can be solved via backward-substitution with only one-row being solved at a time.

### 5.3 Minimization

A Newton update of the form of $\mathbf{H}\partial\mathbf{m} = -\mathbf{g}$ can be obtained by combining Equations 23 and 24. For the least squares data objective function the Newton update has the form

$$(\mathbf{J^T J} + \beta\mathbf{G_w^T G_w})\delta\mathbf{m} = -(\mathbf{J^T}(\mathbf{d(m)} - \mathbf{d_{obs}}) + \beta\mathbf{G_w^T G_w}(\mathbf{m} - \mathbf{m_{ref}})) \quad (30)$$

Although $\mathbf{J}$ does not need to be explicitly formed, every product involves the solution of the block matrix in Equation 28. Solving this system could become prohibitively expensive if a high tolerance solution is required. Due to the approximation of the Hessian the matrix is positive definite and can be solved using Conjugate Gradient (CG). *Dembo et al.* [1982] shows that a high-tolerance solution to the equation is not necessary for convergence. This leads to the inexact Gauss Newton update, where only a few iterations of CG are performed for each model update.

### 5.4 Line Search

After a model update, $\delta\mathbf{m}$, is found, it is incorporated into the current model by

$$\mathbf{m_{k+1}} = \mathbf{m_k} + \alpha_k \delta\mathbf{m} \tag{31}$$

where $\alpha_k$ is the current line search parameter and $\mathbf{m_{k+1}}$ is the new model. The line search parameter is used to control the magnitude of the update. The update must be scaled appropriately so as not to violate the linearization about the current model. Additionally, $\alpha_k$ is systematically decreased such that a sufficient decrease in the objective function is obtained. The sufficient decrease is enforced by a backtracking Armijo line search *Armijo* [1966] where $\alpha_k$ is decreased until the following inequality is satisfied

$$\Phi(\mathbf{m_{k+1}} + \alpha_k \delta\mathbf{m}) \geq \Phi(\mathbf{m_k}) + c_1 \alpha_k \mathbf{g^T} \delta\mathbf{m} \tag{32}$$

where $c_1$ is a constant usually chosen to be quite small (e.g. $10^{-4}$) *Haber* [2011] *Pidlisecky et al.* [2007]; $\mathbf{g}$ is the gradient of the function. This inequality is evaluated iteratively decreasing $\alpha_k$ by a constant $c_2$ each time the inequality is not satisfied; $c_2$ is generally chosen to be between 0.4 and 0.8, with higher values indicating a finer line search and requiring more evaluations of the objective function *Nocedal and Wright* [1999]. Evaluation of the objective function is expensive, and an extensive line search should be avoided. To combat excessive line search iterations, a maximum model update based on $||\delta\mathbf{m}||_\infty$ is chosen, if the model update is larger than this tolerance, it is scaled back. The model update tolerance is chosen by analyzing the problem and setting a maximum change on the model, for example, a two or three order of magnitude change in hydraulic conductivity may be unrealistic. Without scaling $\delta\mathbf{m}$ the model update can be too large and violate parameters in Richards equation leading to problems in evaluating the objective function.

### 5.5 Stopping Criteria

The minimization procedure is repeated with a new linearization until either the norm of the gradient falls below a certain tolerance, the model update is continually small, or the maximum number of iterations have been exhausted. Values for these stopping criteria are often problem dependent *Pidlisecky et al.* [2007]. Running synthetic models that have elements similar to observed data can often give insight into appropriate stopping criteria *Aster et al.* [2004]. A stopping criteria that can be used effectively is the absolute size of the model step *Haber* [2011]. Monitoring the step size can be used to cut-off an inversion when negligible progress is being made. If the updates being added to the model are orders of magnitude smaller than the magnitude of the features of interest, this additional model structure is not of use.Additionally, as discussed briefly in Section 5.4, scaling can be an issue in the gradient of the function, so using it as a valid stopping criteria can be difficult. Testing stopping criteria on synthetic models where the true solution is known, as in this paper, is the best way to understand what stopping criteria to use.

## 6 Preliminary Results & Discussion

The preliminary results for the hydraulic conductivity inverse problem are presented in one-dimension for a two hour infiltration experiment. The soil column is 80cm high and initially dry ($\theta = 0.10$), a constant head boundary condition is enforced at the top of the model of -50cm. Two data points are collected at intervals of 12 minutes at heights of 45cm and 70cm, where 80cm is the top of the soil column. The Van Genuchten parameters are assumed to be known and constant throughout the soil profile, and are the same used by *Celia et al.* [1990] (Figure 1). Additionally, the boundary conditions and initial conditions are assumed to be known. The data is simulated with a synthetic hydraulic conductivity profile and 10% noise is added to the pressure head data recorded at the two locations in the soil column. The pressure head data is shown in Figure 6(a); the pressure head data at 70cm shows an immediate response to the increased pressure head at the top of the model. The data at 45cm, however, decreases over time and may indicate a material with larger pores that cannot hold water under large negative capillary pressures. The inversion is completed on the pressure head data with 10% noise. The true pressure head profile and result of the inversion at all depths is shown in Figure 6(b). There is good correlation over the entire soil profile, with very good correlations at the two recorded data points (45cm and 70cm). The recovered model of hydraulic conductivity is compared to the synthetic model used in Figure 7. The amplitude of the low conductivity layer at 70cm is recovered well, and a higher conductivity layer is found at the depth of 50cm. The reference model used in this inversion was a hydraulic conductivity of $10^{-2}$m/s. Overall, the results of hydraulic conductivity inversion are encouraging as two different layers are recovered with only 22 noisy data points. However, there were many assumptions that would not

be possible in a field situation. For example, boundary and initial conditions may not be known (or may depend on the model). Additionally, the Van Genuchten parameters will change with material properties of the sediment.

The inversion presented here is focused mainly on the methodology. The focus of future work will be on extending this methodology to two- and three-dimensions. Additionally, the formulation of Richards equation presented does not properly simulated saturated environments and an additional time derivative term must be added to the formulation. Incorporating other geophysical data that is sensitive to changes in saturation will be the main focus of future work.

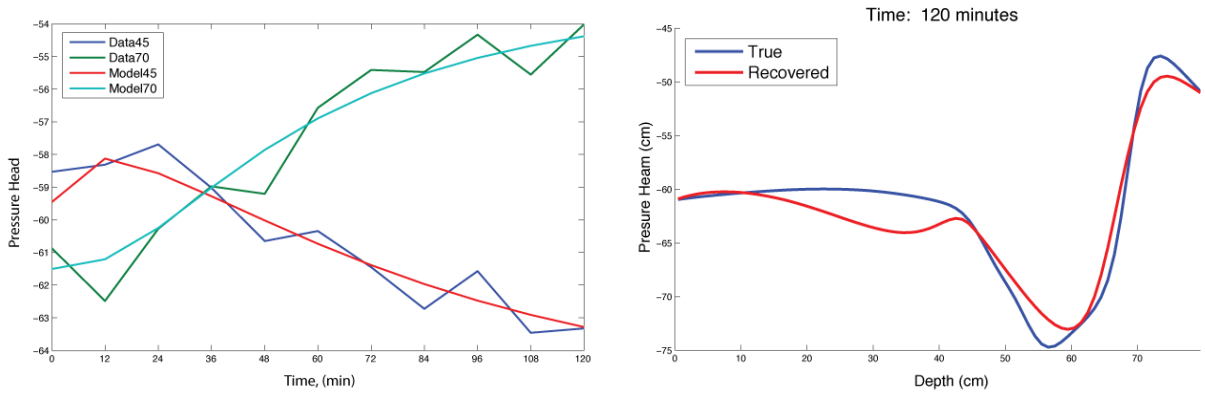


(a) Pressure head data at 45cm and 70cm over time

(b) Pressure head profile at $t = 120$min

Figure 6: Inversion results of pressure head data at recorded locations and the full soil profile.

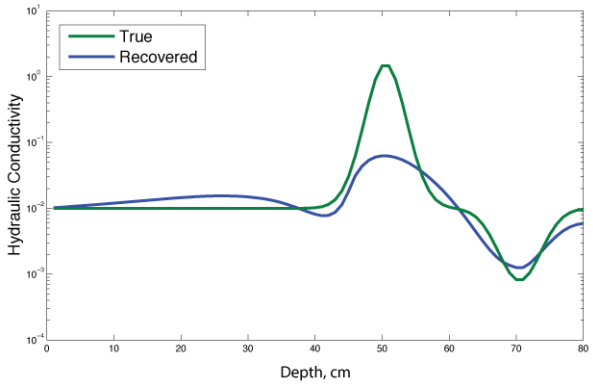


Figure 7: Recovered saturated hydraulic conductivity compared to the synthetic model

## 7 Conclusions

Hydraulic conductivity ($K_s$) is a property of the soil media and is the main regulator of groundwater flow. However, in many hydrogeologic studies $K_s$ is only known as a bulk average. An accurate estimate of saturated hydraulic conductivity that is spatially consistent with the media is highly valuable. Here we have presented an inverse formulation that estimates $K_s$ from time-varying pressure head data. Future work hopes to include saturation data from geophysical imaging that is spatially extensive.

**Acknowledgments**

Eldad Haber provided invaluable guidance and insight into the formulation of the inverse problem. Uri Ascher helped with many of the fundamental challenges in discretizing partial differential equations.

## References

Archie, G., The Electrical Resistivity Log as an Aid in Determining Some Reservoir Characteristics, *Transactions of the AIME*, *146*(1), 54–62, 1942.

Armijo, L., Minimization Of Functions Having Lipschitz Continuous First Partial Derivatives, *Pacific Journal of Mathematics*, *16*(1), 1–3, 1966.

Aster, R. C., B. Borchers, and C. Thurber, *Parameter Estimation and Inverse Problems*, Elsevier Inc., 2004.

Brunone, B., M. Ferrante, N. Romano, and A. Santini, Numerical Simulations of One-Dimensional Infiltration into Layered Soils with the Richards Equation Using Different Estimates of the Interlayer Conductivity, pp. 193–200, 1998.

Celia, M. A., E. T. Bouloutas, and R. L. Zarba, A general mass-conservative numerical solution for the unsaturated flow equation, *Water Resources Research*, *26*(7), 1483–1496, doi:10.1029/WR026i007p01483, 1990.

Dembo, R. S., S. C. Eisenstat, and T. Steihaug, Inexact Newton Methods, *SIAM Journal on Numerical Analysis*, *19*(2), 400–408, doi:10.1137/0719025, 1982.

Haber, E., *Computational Methods for Simulation Based Optimization*, UBC Math, 2011.

Miller, C. T., G. a. Williams, C. T. Kelley, and M. D. Tocci, Robust solution of Richards' equation for nonuniform porous media, *Water Resources Research*, *34*(10), 2599, doi:10.1029/98WR01673, 1998.

Nocedal, J., and S. J. Wright, *Numerical Optimization*, Springer, New York, NY, 1999.

Pidlisecky, A., E. Haber, and R. Knight, RESINVM3D : A 3D resistivity inversion package, *Geophysics*, *72*(2), H1–H10, 2007.

Pidlisecky, A., A. R. Cockett, and R. J. Knight, The Development of Electrical Conductivity Probes for Studying Vadose Zone Processes: Advances in Data Acquisition and Analysis, *Vadose Zone Journal*, *First Look*, doi: 10.2136/vzj2012.0073, 2012.

Tikhonov, A., and V. Arsenin, *Solutions of Ill-Posed Problems*, W.H. Winston and Sons., 1977.

van Genuchten, M. T., A Closed-form Equation for Predicting the Hydraulic Conductivity of Unsaturated Soils, *Soil Science Society of America Journal*, *44*(5), 892, doi:10.2136/sssaj1980.03615995004400050002x, 1980.